

Measuring Trilinear Higgs Coupling in VHH and ZHH Productions at the HL-LHC

Qing-Hong Cao,^{1,2,3,*} Yandong Liu,^{1,†} and Bin Yan^{1,‡}

¹Department of Physics and State Key Laboratory of Nuclear Physics and Technology, Peking University, Beijing 100871, China

²Collaborative Innovation Center of Quantum Matter, Beijing, 100871, China

³Center for High Energy Physics, Peking University, Beijing 100871, China

Determination of trilinear Higgs coupling ($\lambda_{HHH} = \kappa\lambda_{HHH}^{\text{SM}}$) through Higgs pair production is a major motivation for the LHC high luminosity phase. We perform a detailed collider simulation to explore the potential of measuring λ_{HHH} in the VHH ($V = W, Z$) production at the HL-LHC. We find that the trilinear Higgs coupling in the SM ($\lambda_{HHH}^{\text{SM}}$) could be measured at the level of 1.3σ . Combining with the gluon fusion, vector boson fusion and $t\bar{t}HH$ channels, $\lambda_{HHH}^{\text{SM}}$ is expected to be measured at the level of 3.13σ . If no evidence of Higgs pair productions were observed, the VHH production, together with the gluon fusion channel, would impose a bound of $0.5 \leq \kappa \leq 2.2$ at the 95% confidence level.

INTRODUCTION

The trilinear Higgs coupling (λ_{HHH}) is an important parameter of the Higgs boson potential in the Standard Model (SM). Even though λ_{HHH} is related to the Higgs boson mass (m_H) in the SM, it might deviate from the SM value $\lambda_{HHH}^{\text{SM}}$ in new physics (NP) models [1–7]. For example, the deviation of the trilinear Higgs coupling might emerge from non-vanishing higher-dimension operators starting with dimension 6. It is then of critical importance to measure λ_{HHH} to test the SM. Such a goal will only be successful if information from a range of production channels of Higgs boson pairs is included. There are five major channels of Higgs pair productions. Figure 1 plots the inclusive cross sections of all those five channels as a function of κ at the 14 TeV Large Hadron Collider (LHC), where the factor κ is introduced to describe possible NP effects in the trilinear Higgs coupling as $\lambda_{HHH} \equiv \kappa\lambda_{HHH}^{\text{SM}}$. The leading production channel is the so-called gluon fusion (GF) channel, $gg \rightarrow HH$ [8–40], the subleading channel is the vector boson fusion (VBF) process, $qq \rightarrow qqHH$ [9, 11, 19, 41–43], the third channel is $t\bar{t}HH$ production [9, 11, 19, 44, 45], while the last two channels are WHH and ZHH productions [9, 11, 19, 46]. The GF channel has drawn a lot of attentions owing to its large cross section. Searches for Higgs pairs in the decay modes of $b\bar{b}b\bar{b}$, $b\bar{b}\tau\tau$, $b\bar{b}WW$ and $\gamma\gamma b\bar{b}$ have been carried out by the ATLAS collaboration recently [47–49] and a combined upper limit of $\sigma(gg \rightarrow HH) \leq 0.69$ pb is observed. On the other hand, the VBF channel is shown to be less promising to measure the trilinear Higgs coupling [43] as it cannot compete with the process of $gg \rightarrow HHqq$, i.e. high order QCD corrections to the GF channel. The potential of probing λ_{HHH} in the $t\bar{t}HH$ channel at the high-luminosity (HL) LHC (a 14 TeV pp collider with an integrated luminosity of 3000 fb^{-1}) is examined in Refs. [44, 45] which shows that a bound of $\kappa \leq 2.51$ can be reached at 95% CL. Unfortunately, the WHH and ZHH productions are not yet studied carefully in the literature, which is not surprising because

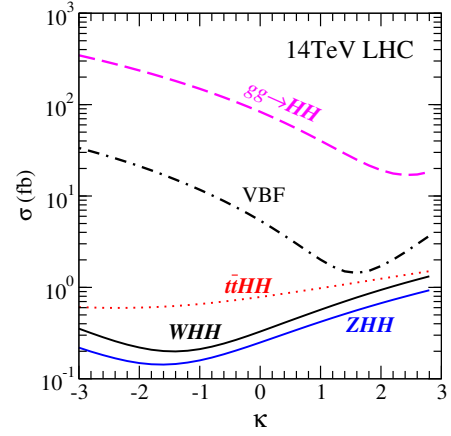


FIG. 1: The production cross section (in unit of fb) of Higgs boson pair production as a function of κ at the 14 TeV LHC.

the VHH production rate are quite small. In this work we focus on the VHH ($V = W^\pm, Z$) production channel and demonstrate that, the VHH production could probe the trilinear Higgs coupling at a comparable level as the GF and $t\bar{t}HH$ channels at the HL-LHC.

The VHH production has many advantages over others production channels. First, the charged lepton and invisible neutrino from W - or Z -boson decays in the VHH production provide a good trigger of signal events. Note that $\sigma(VHH)$ is about one tenth of $\sigma(gg \rightarrow HH)$. However, after including the branching ratio (BR) of V -boson and Higgs boson decays, the cross section of VHH channel is comparable to the GF channel with subsequent decays $HH \rightarrow \gamma\gamma b\bar{b}$. For example,

$$\begin{aligned} \sigma(W^\pm HH) \times \text{BR}(W^\pm \rightarrow \ell^\pm \nu_\ell, HH \rightarrow b\bar{b}b\bar{b}) &= 0.088 \text{fb}, \\ \sigma(ZHH) \times \text{BR}(Z \rightarrow \nu\bar{\nu}, HH \rightarrow b\bar{b}b\bar{b}) &= 0.059 \text{fb}, \\ \sigma(gg \rightarrow HH) \times \text{BR}(HH \rightarrow \gamma\gamma b\bar{b}) &= 0.15 \text{fb}, \end{aligned}$$

where $\ell = e, \mu$. Here, we use the branching ratios at the tree level: $\text{BR}(H \rightarrow b\bar{b}) = 0.83$, $\text{BR}(Z \rightarrow \nu\bar{\nu}) = 0.20$, and $\text{BR}(W^+ \rightarrow \ell^+ \nu_\ell) = 0.11$. Also, the SM backgrounds can be dramatically reduced by tagging the charged lepton

and missing neutrino from the V -boson decay.

Second, all the five channels of Higgs pair productions do not only involve a diagram with λ_{HHH} but also additional contributions which then dilute the sensitivity to λ_{HHH} . The GF channel can be modified by several NP effective operators [24] which might arise from colored NP particles inside the loop diagrams or from the modified top-quark Yukawa coupling, etc. The VHH production could be modified by the HVV anomalous couplings, which are tightly bounded [50, 51].

Last but not least, as depicted in Fig. 1, the dependence of $\sigma(VHH)$ on κ is different from those of the GF, VBF and $t\bar{t}HH$ channels. The $t\bar{t}HH$ production is dominated by the large top Yukawa coupling such that it has a mild dependence on κ . On the other hand, both the GF and the VBF channels are sensitive to a negative κ while the VHH channel is sensitive to a positive κ . One can use the VHH production to probe positive κ and the GF channel to limit negative κ .

The κ dependence can be understood as follows. The GF channel exhibits a large cancellation between the triangle diagram and the box diagram around the threshold of Higgs boson pairs [8]. When $\kappa < 0$ the two diagrams interfere constructively so as to enhance the cross section.

The VBF and VHH channels share the same subprocess of $V^\mu V^\nu \rightarrow HH$ and are related to each other by crossing symmetry. Consider the VBF channel first. The matrix element of $V^\mu(q_1)V^\nu(q_2) \rightarrow H(k_1)H(k_2)$ is

$$M^{\mu\nu} = g^{\mu\nu} \left[\kappa \frac{m_V^2}{v^2} \frac{6m_H^2}{\hat{s} - m_H^2} + \frac{2m_V^2}{v^2} + \frac{4m_V^4}{v^2} \left(\frac{1}{\hat{t} - m_V^2} + \frac{1}{\hat{u} - m_V^2} \right) \right] + \text{others}, \quad (1)$$

where m_V denotes the mass of V -boson and $q_{1,2}$ ($k_{1,2}$) denotes the momentum of the V (Higgs) boson, respectively. Figure 2 shows Feynman diagrams of $V^\mu V^\nu \rightarrow HH$. For the VBF channel, $\hat{s} = (q_1 + q_2)^2$, $\hat{t} = (q_1 - k_1)^2 < 0$ and $\hat{u} = (q_1 - k_2)^2 < 0$. Near the threshold of Higgs boson pairs, $\hat{s} \sim 4m_H^2$ and $\hat{t} \simeq \hat{u} \sim 0$. It gives rise to

$$M^{\mu\nu} \sim \frac{2m_V^2}{v^2} (\kappa - 3) g^{\mu\nu} + \dots,$$

yielding a small cross section around $\kappa \sim +3$ and a large cross section for $\kappa < 0$. The sub-amplitude of VHH production can be obtained from $VV \rightarrow HH$ by crossing one gauge boson from initial state to final state. In the vicinity of the thresholds of HH and VH pairs, $\hat{s} \sim 4m_H^2$ and $\hat{t} = \hat{u} \sim (m_H + m_V)^2$. That yields

$$M^{\mu\nu} \sim \frac{2m_V^2}{v^2} \left(\kappa + 1 + \frac{4m_V^2}{m_H(m_H + 2m_V)} \right) g^{\mu\nu} + \dots,$$

which leads to a small cross section around $\kappa \sim -2$ and a large cross section for $\kappa > 0$.

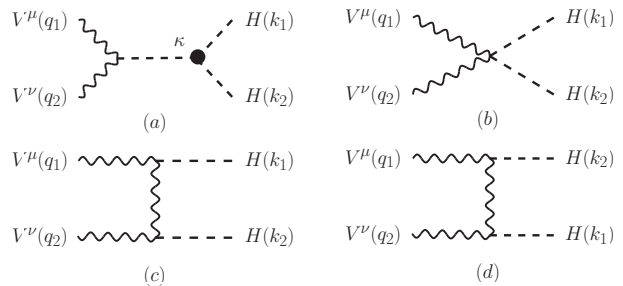


FIG. 2: Feynman diagrams of $V^\mu V^\nu \rightarrow HH$.

Next we perform a collider simulation at the parton level to investigate the sensitivity of the HL-LHC on the λ_{HHH} measurement through the VHH production.

THE WHH PRODUCTION

Our signal consists of both W^+HH and W^-HH productions. The signal and background events are generated with MadEvent [52]. To include higher order QCD corrections, we multiply the cross section of the signal at the tree-level with a factor of $K_{WHH} = 1.39$ [11]. As the production rate is quite small, we demand both the Higgs bosons decay into the $b\bar{b}$ pair which has the largest decay branching ratio among all the decay modes of the Higgs boson. In order to trigger the signal events, we demand a leptonic decay of the W -boson which gives rise to a charged lepton and an invisible neutrino in the final state. The event topology of our signal is characterized by one isolated charged lepton (ℓ^\pm), four b -jets and a large missing transverse momentum (\cancel{E}_T) from the missing neutrino. Both electrons and muons are used in our analysis.

In the article the QCD corrections to the signal processes are taken into account by introducing a constant K factor. It is worthwhile discussing how much our result will be influenced by the QCD corrections. The NNLO QCD corrections to the VHH productions is calculated in Refs. [11], which shows the errors of cross sections are dominated by PDF uncertainty. For example, it shows that the total uncertainty is +3.7% and -3.1% for WHH production, 7.0% and -5.5% for ZHH production at the 14 TeV LHC. The fully differential cross section of WHH production at the next-to-next-to-leading order is calculated in Ref. [53]. It shows the QCD effects mildly modify the transverse momentum distributions of W -boson and the Higgs bosons, which do not alter the acceptance of kinematic cuts used in this study.

The SM backgrounds are rather complicated. In order to reduce the huge SM backgrounds, we require all the four hard jets are tagged as b -jets. In the study we also take into account the possibility that a light quark jet

TABLE I: Numbers of WHH signal ($\kappa = 1$) and background events after a series of cuts which are applied sequentially at the 14 TeV LHC with an integrated luminosity of 3000 fb^{-1} .

	WHH	$Wb\bar{b}b\bar{b}$	$Zb\bar{b}b\bar{b}$	$t\bar{t}$	$t\bar{t}j$	$t\bar{t}H(\rightarrow b\bar{b})$	$t\bar{t}Z(\rightarrow b\bar{b})$	$t\bar{t}b\bar{b}$
Basic cuts	200.9	157770	266580	4.26×10^8	1.0×10^9	296716	97888	7.0×10^6
Selection cuts	34.6	544.4	44.9	3.62×10^7	3.8×10^7	1454.0	442.4	65590.7
4b tagging	7.2	97.2	9.9	767.6	1002	265.1	71.6	922.3
$\chi_{HH} < 1.6$	7.2	2.3	0	170.6	0	45.8	0.1	51.8
$\chi_{tt} > 3.2$	4.8	0.6	0	0	0	20.5	0.05	47.9
m_T & H_T cuts	3.5	0.2	0	0	0	4.1	0	2.0

fakes a b -jet, with mistag efficiency $\epsilon_{j \rightarrow b} = 0.1\%$ with $j = u, d, s$ and $\epsilon_{c \rightarrow b} = 10\%$. The major SM backgrounds include $W^\pm(\rightarrow \ell^\pm \nu_\ell) b\bar{b}b\bar{b}$, $Z(\rightarrow \ell^+ \ell^-) b\bar{b}b\bar{b}$, $t\bar{t}$, $t\bar{t}j$, $t\bar{t}H$, $t\bar{t}Z$ and $t\bar{t}b\bar{b}$. To mimic the signal events, top-quark pairs in the $t\bar{t}$ and $t\bar{t}j$ backgrounds are required to decay into semi-leptonic final states while top-quark pairs in the $t\bar{t}H$, $t\bar{t}Z$ and $t\bar{t}b\bar{b}$ backgrounds decay into dilepton final states. To take into account higher order QCD corrections, we multiply the $t\bar{t}H$ and $t\bar{t}Z$ backgrounds with a factor of $K_{t\bar{t}H} = 1.22$ [54–61] and $K_{t\bar{t}Z} = 1.49$ [60–65], respectively.

When generating both the signal and background events, we impose *basic* cuts as follows: $p_T^{\ell^{\pm, b, j}} > 5$ GeV with $|\eta^{\ell^{\pm, b, j}}| < 5$, where p_T and η denotes the transverse momentum and rapidity, respectively. To get the isolated objects, we require the cone distance $\Delta R_{mn} \equiv \sqrt{(\eta^m - \eta^n)^2 + (\phi^m - \phi^n)^2}$ between the object m and n is at least 0.4. The numbers of signal and background events are shown in the second row of Table I.

There are also many other SM backgrounds involving light non- b jets, e.g. $Wb\bar{b}c\bar{c}$ (5.6 fb), $Wc\bar{c}c\bar{c}$ (3.8 fb), $Wb\bar{b}jj$ ($\sim 10^3$ fb), $Wc\bar{c}jj$ ($\sim 10^3$ fb), $Wjjjj$ ($\sim 10^5$ fb), WWZ (95.9 fb), ZZZ (10.4 fb), WZZ (30.2 fb), WWW (12.6 fb) and $t\bar{t}ZZ$ (1.8 fb). The numbers shown inside the bracket denote the production cross section after imposing $p_T^{b, j} \geq 40$ GeV with $|\eta^{b, j}| \leq 2.5$. All the above light-jet backgrounds can be safely ignored after tagging four b -jets. For example, $\sigma(WWZ \rightarrow \ell^\pm b\bar{b}b\bar{b} + \cancel{E}_T) \sim 10^{-5}$ fb, $\sigma(ZZZ \rightarrow \ell^\pm b\bar{b}b\bar{b} + \cancel{E}_T) \sim 10^{-3}$ fb. From now on we ignore those light-jet backgrounds in our collider simulations.

At the analysis level, all the signal and background events are required to pass a set of *selection* cuts [48]:

$$p_T^e \geq 15 \text{ GeV}, \quad p_T^\mu \geq 10 \text{ GeV}, \quad p_T^b \geq 40 \text{ GeV},$$

$$|\eta^{e, \mu, b}| \leq 2.5, \quad \Delta R_{bb, bl} > 0.4, \quad \cancel{E}_T \geq 40 \text{ GeV}. \quad (2)$$

We model detector resolution effects by smearing the final state energy according to $\delta E/E = \mathcal{A}/\sqrt{E/\text{GeV}} \oplus \mathcal{B}$, where we take $\mathcal{A} = 10(85)\%$ and $\mathcal{B} = 1(5)\%$ for leptons(jets). We demand only one charged lepton and four hard jets in the central region of the detector. Those reducible backgrounds with more jets or charged leptons could mimic the experimental signature of the signal

events if the p_T of additional jets or leptons is less than 10 GeV or its rapidity (in magnitude) is larger than 3.5. As shown in the third row of Table I, roughly 1/6 of the signal events pass the selection cuts.

Once the four jets are trigged, one can require them to be b -jets. That significantly reduces the SM backgrounds consisting of light jets; see the fourth row of Table I. The b -tagging efficiency depends on both p_T^b and η^b . We adapt the b -tagging efficiency given in Ref. [24] which yields on average a b -tagging efficiency of 70% in our analysis.

The four b -jets in the signal events originate from the Higgs boson decay. We first order the jets by their values of p_T and then demand at least one combination of the four jets to be consistent with those expected for the $HH \rightarrow b\bar{b}b\bar{b}$ decay, i.e.

$$\chi_{HH} \equiv \sqrt{\left(\frac{m_{ij} - m_H}{\sigma_{m_H}}\right)^2 + \left(\frac{m_{i'j'} - m_H}{\sigma_{m_H}}\right)^2} \leq 1.6, \quad (3)$$

where m_{ij} denotes the invariant mass of the dijet i and j , and $\sigma_{m_H} (= m_H/10)$ is the dijet mass resolution. All the signal events pass the cut while only 1% of the background events remains.

At this stage of analysis, the dominant background is from $t\bar{t}$ production. Following the ATLAS study [48], we check the compatibility with top-quark decay hypothesis with the following variable

$$\chi_{tt} = \sqrt{\left(\frac{\tilde{m}_W - m_W}{\sigma_{m_W}}\right)^2 + \left(\frac{\tilde{m}_t - m_t}{\sigma_{m_t}}\right)^2}, \quad (4)$$

with $m_W = 80.419$ GeV and $m_t = 173$ GeV. The $\sigma_{m_W} = 0.1m_W$ and $\sigma_{m_t} = 0.1m_t$ represent the dijet and three-jet system mass resolutions, \tilde{m}_W and \tilde{m}_t are the invariant mass of the W and top candidates. If either dijet in an event has $\chi_{tt} \leq 3.2$ for any possible combination with an extra jet, the event is rejected. This requirement sufficiently reduces the $t\bar{t}$ background, whilst retaining $\sim 67\%$ of signal events; see the sixth row of Table I.

While the \cancel{E}_T in the signal events arises mainly from the missing neutrinos, that in the background events is contaminated by jets or leptons either falling into a

TABLE II: The numbers of ZHH ($\kappa = 1$) signal and background events after a series of cuts which are applied sequentially at the 14 TeV LHC with an integrated luminosity of 3000 fb^{-1} .

	ZHH	$Zb\bar{b}b\bar{b}$	$Zb\bar{b}c\bar{c}$	$Zcc\bar{c}\bar{c}$	$ZZ(\rightarrow b\bar{b})b\bar{b}$	$t\bar{t}c\bar{c}$	$t\bar{t}b\bar{b}$	$t\bar{t}Z(\rightarrow b\bar{b})$	$t\bar{t}H(\rightarrow b\bar{b})$	$t\bar{t}$	$t\bar{t}j$
Basic cuts	155.4	1.2×10^6	3.2×10^6	2.0×10^6	24627	4.6×10^6	7.0×10^6	97889	296716	4.3×10^8	1.0×10^9
Selection cuts	23.2	2589.6	4504.8	2000.4	308.0	2131.3	2435.0	11.4	29.4	1.4×10^6	1.4×10^6
$4b$ tagging	4.8	499.4	19.2	0	56.6	0	27.7	2.0	3.6	28.4	66.8
$\chi_{HH} < 1.6$	4.8	10.8	0	0	0.1	0	0	0.05	0.7	0	0

large rapidity region or carrying a too small transverse momentum to be detected. To further suppress the SM backgrounds, we impose cuts on the transverse mass (m_T) of \cancel{E}_T and charged lepton, $m_T(\ell^\pm, \cancel{E}_T) = \sqrt{2p_T^\ell \cancel{E}_T (1 - \cos \phi)}$ with ϕ being the azimuthal angle between ℓ^\pm and \cancel{E}_T , and H_T defined as the scalar sum of p_T 's of jets and charged lepton as follows:

$$m_T \leq m_W, \quad H_T \geq 400 \text{ GeV}. \quad (5)$$

The SM backgrounds are suppressed efficiently such that only 6.3 background events survive after all the cuts. We end up with 3.5 signal events.

Equipped with the optimal cuts shown above, we vary κ to obtain a 5 standard deviations (σ) statistical significance using

$$\sqrt{-2 \left[(n_b + n_s) \log \frac{n_b}{n_s + n_b} + n_s \right]}, \quad (6)$$

from which we obtain a 5σ discovery significance requires $\kappa \geq 4.81$ or $\kappa \leq -7.68$. Here, n_b and n_s represents the numbers of the signal and background events, respectively. A discovery significance of the SM trilinear Higgs coupling ($\kappa = 1$) is found to be around 1.29σ , which is comparable to the projected significance derived from the GF channel by the ATLAS (1.19σ) [66] and CMS collaborations (1.65σ) [67].

In the case that no evidence of Higgs pair production is observed, one can set a 2σ exclusion limit on κ from

$$\sqrt{-2 \left[n_b \log \frac{n_s + n_b}{n_b} - n_s \right]} = 2, \quad (7)$$

yielding $-5.11 \leq \kappa \leq 2.24$.

THE ZHH PRODUCTION

Now consider the ZHH production. We require that both the Higgs bosons decay into the $b\bar{b}$ pair and the Z boson decays into neutrinos. The topology of our signal events is characterized by four b -jets and a large \cancel{E}_T from the missing neutrinos. The major SM backgrounds are

$$Zb\bar{b}b\bar{b}, Zb\bar{b}c\bar{c}, Zcc\bar{c}\bar{c}, ZZ(\rightarrow b\bar{b})b\bar{b}, t\bar{t}c\bar{c}, t\bar{t}b\bar{b}, t\bar{t}Z(\rightarrow b\bar{b}), t\bar{t}H(\rightarrow b\bar{b}), t\bar{t}, t\bar{t}j.$$

Top quark pairs in the $t\bar{t}$ and $t\bar{t}j$ backgrounds are demanded to decay into semi-leptonic final states, while those pairs in the $t\bar{t}c\bar{c}$, $t\bar{t}b\bar{b}$, $t\bar{t}Z$ and $t\bar{t}H$ backgrounds decay into both semi-leptonic and dilepton final states. The background $t\bar{t}Z$ with $Z \rightarrow \nu\bar{\nu}$ is negligible after requiring four b -tagged jets.

The cross section of the signal is normalized to the NNLO precision [11] while the $t\bar{t}H$ and $t\bar{t}Z$ backgrounds to the NLO accuracy [54–65]. We also consider a few SM backgrounds involving light jets, e.g. ZZZ (10.4 fb), WZZ (30.2 fb), $Zjjjj$ ($\sim 10^4$ fb), $Zb\bar{b}jj$ ($\sim 10^3$ fb), $Zc\bar{c}jj$ ($\sim 10^3$ fb), $WZb\bar{b}$ (18 fb) and $t\bar{t}jj$ ($\sim 10^5$ fb). The numbers shown inside the bracket denote the production cross section after imposing $p_T^{b,j} \geq 40$ GeV with $|\eta^{b,j}| \leq 2.5$ on the jets. Again we note that those light flavor jet backgrounds are negligible after requiring four b -tagged jets in the final state.

The *selection* cuts used in the ZHH production are the same as those used in the WHH channel (see Eq. 2) except that now we demand $\cancel{E}_T > 100$ GeV to trigger the events. Table II displays the numbers of signal ($\kappa = 1$) and background events after the selection cuts. For the four b -tagged jets, we also demand $\chi_{HH} < 1.6$ which sufficiently suppresses the backgrounds. We end up with 4.8 signal events and 11.7 background events. Based on Eqs. 6 and 7, we obtain a 5σ discovery significance and 2σ exclusion limits on κ , respectively. It shows that the 5σ significance requires $\kappa \geq 4.85$ or $\kappa \leq -8.10$, while the 2σ exclusion bound is $-5.42 \leq \kappa \leq 2.16$. The discovery significance of λ_{HH}^{SM} is 1.32σ in the ZHH channel which is comparable to that of the GF channel.

TABLE III: The sensitivity to $\lambda_{HHH} = \kappa \lambda_{HHH}^{\text{SM}}$ in several production channels of Higgs boson pairs at the HL-LHC.

	SM ($\kappa = 1$)	5σ discovery potential	2σ exclusion bound
WHH	1.29σ	$\kappa \leq -7.7, \kappa \geq 4.8$	$-5.1 \leq \kappa \leq 2.2$
ZHH	1.32σ	$\kappa \leq -8.1, \kappa \geq 4.8$	$-5.4 \leq \kappa \leq 2.2$
GF($b\bar{b}\gamma\gamma$) [66]	1.19σ	$\kappa \leq -4.5, \kappa \geq 8.1$	$-0.2 \leq \kappa \leq 4.9$
GF($b\bar{b}\gamma\gamma$) [67]	1.65σ	$\kappa \leq -2.6, \kappa \geq 6.3$	$0.5 \leq \kappa \leq 4.1$
VBF [43]	0.59σ	$\kappa \leq -1.7, \kappa \geq 5.0$	$-0.4 \leq \kappa \leq 3.5$
$t\bar{t}HH$ [44, 45]	1.38σ	$\kappa \leq -11.4, \kappa \geq 6.9$	$-7.2 \leq \kappa \leq 2.5$

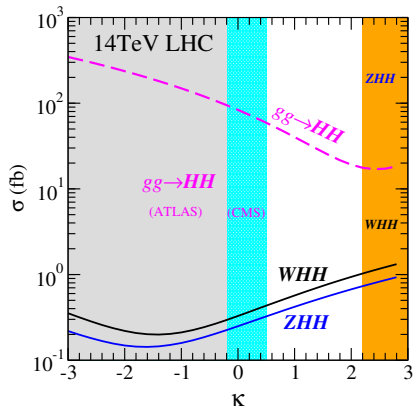


FIG. 3: The 95% exclusion bounds on $\lambda_{HHH} = \kappa\lambda_{HHH}^{\text{SM}}$ derived from the VHH and GF channels at the HL-LHC.

DISCUSSIONS AND CONCLUSIONS

The sensitivity to the trilinear Higgs coupling is summarized in Table III. The $\lambda_{HHH}^{\text{SM}}$ can be probed at the level of 1.32σ (1.29σ) in the ZHH (WHH) production at the HL-LHC, respectively. The discovery potential of the VHH production is comparable to those of the GF channel given by the ATLAS collaboration (1.19σ) [66] and CMS collaboration (1.65σ) [67] and $t\bar{t}HH$ production (1.38σ) [44, 45]. The VBF channel can probe $\lambda_{HHH}^{\text{SM}}$ only at the level of 0.59σ [43]. In order to combine all the channels to probe the Higgs trilinear coupling, we use the following significance formula [68],

$$\sqrt{-2 \log \left(\prod_{i=1}^N \frac{L(b_i | s_i + b_i)}{L(s_i + b_i | s_i + b_i)} \right)}, \quad (8)$$

where s_i and b_i denotes the number of signal and background events after imposing a set of cuts in the production channel i , respectively. The likelihood function is defined as $L(x_i | n_i) = x_i^{n_i} e^{-x_i} / n_i!$. The $\lambda_{HHH}^{\text{SM}}$ can be measured at the level of 3.13σ after combining all the above five channels.

The trilinear Higgs coupling might be modified sizeably in NP models. We vary κ to estimate the value of λ_{HHH} needed for a 5σ significance for each HH production channel; see the third column in Table III.

If no evidence of Higgs pair productions were observed, one could set a 2σ exclusion limit on κ for each HH production channel; see the fourth column in Table III. Figure 3 displays the 2σ exclusion regions on κ from the GF channel (gray band from the ATLAS study and cyan band from the CMS result) and from the WHH and ZHH productions (orange band). The most stringent lower limit and upper limit on κ arises from the GF channel and the VHH production, respectively, which requires $0.5 \leq \kappa \leq 2.2$ at the 95% confidence level.

The work is supported in part by the National Science

Foundation of China under Grand No. 11275009, 11675002 and 11635001.

* Electronic address: qinghongcao@pku.edu.cn

† Electronic address: ydliu@pku.edu.cn

‡ Electronic address: binyan@pku.edu.cn

- [1] S. Kanemura, S. Kiyoura, Y. Okada, E. Senaha, and C. P. Yuan, Phys. Lett. **B558**, 157 (2003), hep-ph/0211308.
- [2] T. Han, H. E. Logan, B. McElrath, and L.-T. Wang, Phys. Rev. **D67**, 095004 (2003), hep-ph/0301040.
- [3] S. Kanemura, Y. Okada, E. Senaha, and C. P. Yuan, Phys. Rev. **D70**, 115002 (2004), hep-ph/0408364.
- [4] B. Bhattacharjee and A. Choudhury, Phys. Rev. **D91**, 073015 (2015), 1407.6866.
- [5] V. Barger, L. L. Everett, C. B. Jackson, A. D. Peterson, and G. Shaughnessy, Phys. Rev. **D90**, 095006 (2014), 1408.2525.
- [6] B. Hespel, D. Lopez-Val, and E. Vryonidou, JHEP **09**, 124 (2014), 1407.0281.
- [7] L. Wu, J. M. Yang, C.-P. Yuan, and M. Zhang, Phys. Lett. **B747**, 378 (2015), 1504.06932.
- [8] E. W. N. Glover and J. J. van der Bij, Nucl. Phys. **B309**, 282 (1988).
- [9] M. Moretti, S. Moretti, F. Piccinini, R. Pittau, and A. D. Polosa, JHEP **02**, 024 (2005), hep-ph/0410334.
- [10] S. Dawson, E. Furlan, and I. Lewis, Phys. Rev. **D87**, 014007 (2013), 1210.6663.
- [11] J. Baglio, A. Djouadi, R. Grber, M. M. Mhleitner, J. Quevillon, and M. Spira, JHEP **04**, 151 (2013), 1212.5581.
- [12] A. Papaefstathiou, L. L. Yang, and J. Zurita, Phys. Rev. **D87**, 011301 (2013), 1209.1489.
- [13] M. J. Dolan, C. Englert, and M. Spannowsky, JHEP **10**, 112 (2012), 1206.5001.
- [14] D. Y. Shao, C. S. Li, H. T. Li, and J. Wang, JHEP **07**, 169 (2013), 1301.1245.
- [15] F. Goertz, A. Papaefstathiou, L. L. Yang, and J. Zurita, JHEP **06**, 016 (2013), 1301.3492.
- [16] Q. Li, Q.-S. Yan, and X. Zhao, Phys. Rev. **D89**, 033015 (2014), 1312.3830.
- [17] C.-Y. Chen, S. Dawson, and I. M. Lewis, Phys. Rev. **D90**, 035016 (2014), 1406.3349.
- [18] C.-R. Chen and I. Low, Phys. Rev. **D90**, 013018 (2014), 1405.7040.
- [19] R. Frederix, S. Frixione, V. Hirschi, F. Maltoni, O. Mattelaer, P. Torrielli, E. Vryonidou, and M. Zaro, Phys. Lett. **B732**, 142 (2014), 1401.7340.
- [20] F. Maltoni, E. Vryonidou, and M. Zaro, JHEP **11**, 079 (2014), 1408.6542.
- [21] Q. Li, Z. Li, Q.-S. Yan, and X. Zhao, Phys. Rev. **D92**, 014015 (2015), 1503.07611.
- [22] S. Dawson, A. Ismail, and I. Low, Phys. Rev. **D91**, 115008 (2015), 1504.05596.
- [23] H.-J. He, J. Ren, and W. Yao (2015), 1506.03302.
- [24] Q.-H. Cao, B. Yan, D.-M. Zhang, and H. Zhang (2015), 1508.06512.
- [25] D. de Florian and J. Mazzitelli, Phys. Rev. Lett. **111**, 201801 (2013), 1309.6594.
- [26] D. de Florian and J. Mazzitelli, JHEP **09**, 053 (2015), 1505.07122.

- [27] S. Dawson, S. Dittmaier, and M. Spira, *Phys. Rev.* **D58**, 115012 (1998), hep-ph/9805244.
- [28] D. de Florian and J. Mazzitelli, *Phys. Lett.* **B724**, 306 (2013), 1305.5206.
- [29] J. Grigo, J. Hoff, K. Melnikov, and M. Steinhauser, *Nucl. Phys.* **B875**, 1 (2013), 1305.7340.
- [30] R. Grober, M. Muhlleitner, M. Spira, and J. Streicher, *JHEP* **09**, 092 (2015), 1504.06577.
- [31] J. Grigo, K. Melnikov, and M. Steinhauser, *Nucl. Phys.* **B888**, 17 (2014), 1408.2422.
- [32] A. Azatov, R. Contino, G. Panico, and M. Son, *Phys. Rev.* **D92**, 035001 (2015), 1502.00539.
- [33] R. Contino, M. Ghezzi, M. Moretti, G. Panico, F. Piccinini, and A. Wulzer, *JHEP* **08**, 154 (2012), 1205.5444.
- [34] T. Plehn, M. Spira, and P. M. Zerwas, *Nucl. Phys.* **B479**, 46 (1996), [Erratum: *Nucl. Phys.*B531,655(1998)], hep-ph/9603205.
- [35] K. Nishiwaki, S. Niyogi, and A. Shivaji, *JHEP* **04**, 011 (2014), 1309.6907.
- [36] M. Slawinska, W. van den Wollenberg, B. van Eijk, and S. Bentvelsen (2014), 1408.5010.
- [37] A. J. Barr, M. J. Dolan, C. Englert, and M. Spannowsky, *Phys. Lett.* **B728**, 308 (2014), 1309.6318.
- [38] V. Barger, L. L. Everett, C. B. Jackson, and G. Shaughnessy, *Phys. Lett.* **B728**, 433 (2014), 1311.2931.
- [39] D. E. Ferreira de Lima, A. Papaefstathiou, and M. Spannowsky, *JHEP* **08**, 030 (2014), 1404.7139.
- [40] D. Wardrope, E. Jansen, N. Konstantinidis, B. Cooper, R. Falla, and N. Norjoharuddeen, *Eur. Phys. J.* **C75**, 219 (2015), 1410.2794.
- [41] M. J. Dolan, C. Englert, N. Greiner, and M. Spannowsky, *Phys. Rev. Lett.* **112**, 101802 (2014), 1310.1084.
- [42] L.-S. Ling, R.-Y. Zhang, W.-G. Ma, L. Guo, W.-H. Li, and X.-Z. Li, *Phys. Rev.* **D89**, 073001 (2014), 1401.7754.
- [43] M. J. Dolan, C. Englert, N. Greiner, K. Nordstrom, and M. Spannowsky, *Eur. Phys. J.* **C75**, 387 (2015), 1506.08008.
- [44] C. Englert, F. Krauss, M. Spannowsky, and J. Thompson, *Phys. Lett.* **B743**, 93 (2015), 1409.8074.
- [45] T. Liu and H. Zhang (2014), 1410.1855.
- [46] V. D. Barger, T. Han, and R. J. N. Phillips, *Phys. Rev.* **D38**, 2766 (1988).
- [47] G. Aad et al. (ATLAS), *Phys. Rev. Lett.* **114**, 081802 (2015), 1406.5053.
- [48] G. Aad et al. (ATLAS), *Eur. Phys. J.* **C75**, 412 (2015), 1506.00285.
- [49] G. Aad et al. (ATLAS) (2015), 1509.04670.
- [50] CMS Collaboration (2015), CMS-PAS-HIG-15-002.
- [51] The ATLAS and CMS Collaborations (2015), ATLAS-CONF-2015-044.
- [52] J. Alwall, M. Herquet, F. Maltoni, O. Mattelaer, and T. Stelzer, *JHEP* **06**, 128 (2011), 1106.0522.
- [53] H. T. Li and J. Wang, *Phys. Lett.* **B765**, 265 (2017), 1607.06382.
- [54] W. Beenakker, S. Dittmaier, M. Kramer, B. Plumper, M. Spira, and P. M. Zerwas, *Phys. Rev. Lett.* **87**, 201805 (2001), hep-ph/0107081.
- [55] W. Beenakker, S. Dittmaier, M. Kramer, B. Plumper, M. Spira, and P. M. Zerwas, *Nucl. Phys.* **B653**, 151 (2003), hep-ph/0211352.
- [56] S. Dawson, L. H. Orr, L. Reina, and D. Wackerroth, *Phys. Rev.* **D67**, 071503 (2003), hep-ph/0211438.
- [57] S. Dawson, C. Jackson, L. H. Orr, L. Reina, and D. Wackerroth, *Phys. Rev.* **D68**, 034022 (2003), hep-ph/0305087.
- [58] Y. Zhang, W.-G. Ma, R.-Y. Zhang, C. Chen, and L. Guo, *Phys. Lett.* **B738**, 1 (2014), 1407.1110.
- [59] S. Frixione, V. Hirschi, D. Pagani, H. S. Shao, and M. Zaro, *JHEP* **09**, 065 (2014), 1407.0823.
- [60] F. Maltoni, D. Pagani, and I. Tsinikos (2015), 1507.05640.
- [61] S. Frixione, V. Hirschi, D. Pagani, H. S. Shao, and M. Zaro, *JHEP* **06**, 184 (2015), 1504.03446.
- [62] A. Lazopoulos, T. McElmurry, K. Melnikov, and F. Petriello, *Phys. Lett.* **B666**, 62 (2008), 0804.2220.
- [63] M. V. Garzelli, A. Kardos, C. G. Papadopoulos, and Z. Trocsanyi, *Phys. Rev.* **D85**, 074022 (2012), 1111.1444.
- [64] A. Kardos, Z. Trocsanyi, and C. Papadopoulos, *Phys. Rev.* **D85**, 054015 (2012), 1111.0610.
- [65] M. V. Garzelli, A. Kardos, C. G. Papadopoulos, and Z. Trocsanyi, *JHEP* **11**, 056 (2012), 1208.2665.
- [66] ATLAS Collaboration, Tech. Rep. ATLAS-PHYS-PUB-2014-019, CERN, Geneva (2014).
- [67] CMS Collaboration (2015), CMS-PAS-FTR-15-002.
- [68] G. Cowan, K. Cranmer, E. Gross, and O. Vitells, *Eur. Phys. J.* **C71**, 1554 (2011), [Erratum: *Eur. Phys. J.*C73,2501(2013)], 1007.1727.